ORNL/TM-2000/285

Thermal Conductivity of IONSIV® IE-911™ Crystalline Silicotitanate and Savannah River Waste Simulant Solutions

Barry B. Spencer
Hsin Wang
Kimberly K. Anderson

ORNL/TM-2000/285

Chemical Technology Division

Thermal Conductivity of IONSIV® IE-911™ Crystalline Silicotitanate and Savannah River Waste Simulant Solutions

Barry B. Spencer*
Hsin Wang†
Kimberly K. Anderson

*Robotics and Process Systems Division, ORNL
†Metals and Ceramics Division, ORNL

Date Published: November 2000

Prepared by
OAK RIDGE NATIONAL LABORATORY
Oak Ridge, Tennessee 37831-6285
managed by
UT-BATTELLE, LLC
for the
U.S. DEPARTMENT OF ENERGY
under contract DE-AC05-00OR22725

CONTENTS

LIST OF FIGURES

LIST OF TABLES

ABSTRACT

The thermal conductivities of crystalline silicotitanate (CST)–air and CST–average simulant mixtures were measured over temperature ranges of 20 to 130°C and 23 to 65°C, respectively. The void fraction of granulated CST was also measured because this parameter is important in predicting the thermal conductivity of two-phase mixtures from the thermal conductivities of the component parts.

The thermal conductivity of CST-air mixtures increased linearly with increasing temperature. Methods available in the literature to estimate the thermal conductivity of two-phase mixtures from the conductivities of the components were used to back-calculate the thermal conductivity of the solid phase. The conductivity of the solid phase also varied nearly linearly with temperature.

A limited number of measurements of the thermal conductivity of CST-simulant mixtures were made. The tendency of water to evaporate rapidly from the mixture, resulting in crystallization of the salts, limited the upper temperature at which thermal conductivity could be measured. Literature methods are available to estimate the thermal conductivity of aqueous ionic solutions. Results of these calculations were combined with the measured thermal conductivity of the solid phase to estimate the conductivity of CST–average simulant mixtures. The experimentally measured thermal conductivity of the mixture compared reasonably well with the calculations.

Latent heat effects associated with adsorbed water or waters of hydration were observed. The information made it clear that measurements of thermal conductivity of wet CST (i.e., immersed and then drained of the bulk liquid) would be compromised.

1. INTRODUCTION

1.1 Background

Crystalline silicotitanate (CST) is being investigated as an inorganic ion-exchange medium to remove cesium from the supernatant stored in the high-level radioactive waste tanks at the Savannah River Site (SRS). This report partially fulfills the requirements of the Technical Task Request (TTR), HLW-SDT-TTR-99-32.2, Rev. 0, item 32.2.2 (Jacobs, 1999) as described in the Technical Task Plan (TTP), ORNL/CF-99/68 (Spencer, 2000).

The supernatant is primarily a mixture of aqueous sodium nitrate and sodium hydroxide, with smaller concentrations of other species. The total sodium concentration is ~ 5.6 *M*. Although the cesium concentration is low, $<1.4 \times 10^{-4}$ *M*, the ^{137}Cs accounts for much of the radioactivity of the supernatant. Sorption of the cesium from the supernatant results in the concentration of the ^{137}Cs into the much smaller volume of the CST bed. In concentrated form, the ^{137}Cs becomes a compact source of significant thermal energy (~4.95 W/1000 Ci). Engineering designs of the CST sorption column must handle this thermal load; otherwise, hot spots could develop within the column and degrade the performance of the ion-exchange process. Development of adequate mathematical models to aid the design of the CST ion-exchange column requires information on the thermal properties of the CST. The heat capacity has been measured (Bostick and Steele, 1999), but data on thermal conductivity are lacking.

The commercial source of the granular form of CST is UOP Molecular Sieves, LLC, Mt. Laurel, New Jersey. It is sold under the trade name IONSIV® IE-911™. The objective is to measure the effective thermal conductivity of IE-911™.

1.2 Rationale for Selecting Measurement Conditions

In one of several viable alternatives, the equipment implemented to remove ^{137}Cs from tank waste supernatant is a simple vertical tube filled with granular CST – that is, an ion-exchange column. During normal operation of the column, liquid supernatant flows downward through the porous bed of CST granules. In this mode of operation, heat generated by radioactive decay of sorbed ^{137}Cs is transferred from the solid particles to

the liquid phase. The particle size of the CST is very small (average particle diameter of ~400 μm). Should the thermal conductivity of the individual solid particle be poor, a large temperature difference between the surface and center of the particle is unlikely to arise, because of the small distance involved. It may be surmised that convective heat transfer dominates the temperature variations within the column under normal circumstances.

Radiolysis of water in the column will produce free hydrogen and oxygen gas. Production of bubbles within the bed displaces the liquid, leaving a zone of wetted particles with most of the interstitial voids filled with hydrogen and oxygen gas. Prior tests (Welch et al., 2000) have shown that small bubbles move through the column. Because these bubble are rapidly replaced with liquid, they probably have little effect on the temperature gradients. The column retains a steady-state void fraction of ~7%, and some larger bubbles were observed to adhere to the wall of the column. Retained and immobile bubbles represent locations in the column where cooling by the flowing supernatant is interrupted. Heat transfer in these zones is limited by thermal conductivity.

If the liquid flow is halted, then the mode of heat transfer changes character. The bed of granulated material tends to stabilize the liquid with respect to natural convection; as a result, the liquid remains quiescent. The contents of the column must be cooled from the outer surfaces or with heat-exchange tubes imbedded in the bed of particles. Heat transfer is limited by the thermal conductivity of the heterogeneous solid-liquid medium (solid particles with the interstitial voids filled with liquid). If a localized hot spot develops so that the temperature approaches the boiling point of the liquid (probable range of 100 to ~120°C), then the expanding water vapor can displace the fluid, leaving a wetted zone of particles (solid particles wetted with the liquid but with most of the interstitial voids filled with water vapor). This is similar to voids caused by noncondensable radiolysis products. Prolonged heating will cause the water to fully evaporate from the particles, leaving precipitated salts on the particles with the interstitial voids filled with water vapor.

Three general physical conditions in which thermal conductivity controls the removal of heat from the ion-exchange column appear to exist. Within these general conditions, subsets of specific chemical makeup can be identified.

1.2.1 Dry Solid Particles

A dry solids bed may result when the water in a wetted bed completely evaporates (not counting waters of hydration). A drained bed of solids retains only a fraction of the liquid associated with an immersed bed. When the water is removed, the crystallized salts remaining are a small fraction of the mass of the CST granules. The crystallized solids coat the granule with little effect, but solids that crystallize within the pores of individual CST grains might cause more substantial effects on the thermal conductivity of an individual grain.

1.2.2 Immersed Solid Particles

In this condition, the solids bed is submerged in the liquid. For practical purposes, all the fluid within the interstitial bed of solid particles may be considered the liquid phase. The thermal conductivity of the supernatant simulant has been measured at 19°C in previous studies (Bostick and Steele, 1999). Data are not available on the thermal conductivity of the solid particles.

1.2.3 Wetted Solid Particles

A wetted solids bed is formed when the liquid is displaced by a gas. The liquid may be displaced by radiolytically produced noncondensable gas or by thermally produced water vapor (steam). Most of the interstitial void space of the solids bed is filled with the gas, and the particles themselves are coated with a thin film of liquid. This condition may be simulated by draining the liquid from an immersed solids bed, for example, by gravity filtration of the solids on a frit. Two subsets of this condition are evident: one in which the gas is a mixture of hydrogen and oxygen and another in which the gas is water vapor. The thermal conductivities of these gases are available from the literature.

1.3 Objectives

No data are available on the thermal conductivity of IE-911™. The thermal conductivity of the supernatant simulant has been measured and reported (Bostick and

Steele, 1999). It is anticipated that the effective thermal conductivity of the granular CST will be strongly dependent on the properties of the fluid that fills the interstitial voids.

The objectives are to measure the effective thermal conductivity in up to three conditions: (1) granular CST that has been treated for use in the ion-exchange column and then dried; (2) the same material used in item 1 but immersed in supernatant simulant; and, optionally, (3) the same material used in item 2 with the liquid supernatant gravity filtered from the solid.

In the first test, the interstitial voids of the dry granular CST will be filled with air. The thermal properties of air are known, so simple models may be developed to separate the thermal conductivity of the solid from the measured value of the mixture. In operating columns, gases likely to fill the interstitial voids of dry CST are water vapor, hydrogen, oxygen, and mixtures of these three gases. The properties of these gases are also known, and the thermal conductivity varies within a small range. Based on measurements made in air, computation of the effective thermal conductivity for systems with different interstitial gases should yield acceptable results.

In the second test, the effective thermal conductivity of IE-911™ immersed in simulant will be measured experimentally. The value will be estimated theoretically from the measurements made in the first test and the previously reported thermal conductivity of supernatant simulant. The experimental and calculated values will be compared.

The third test is optional, and the decision to proceed with it will depend on the outcome of the first two tests. In that test, a similar measurement of the effective thermal conductivity of IE-911™, wetted with simulant and gravity drained of bulk liquid, will be performed. The interstitial gas will be air. Thermal conductivities of drained solids with interstitial gases other than air may be computed from the properties of those other gases.

2. LITERATURE REVIEW AND ANALYSIS

2.1 Methods to Calculate Thermal Conductivity of Porous Media

A general method of calculating the effective thermal conductivity of porous or granulated media is given by Perry and Chilton (1973). The method makes use of the Russell equation (Russell, 1935), which calculates the thermal conductivity of a two-phase mixture from the thermal conductivity of the individual components. The formula is

$$\frac{k_{\text{comp}}}{k_{\text{cont}}} = \frac{\nu\ p^{2/3} + 1 - p^{2/3}}{\nu\,(p^{2/3} - p) + 1 - p^{2/3} + p}\ , \tag{2.1}$$

where

k = thermal conductivity,

"comp" denotes values for the composite mixture,

"cont" denotes values for the continuous phase,

p = the porosity (volume fraction of voids or obstacles),

ν = ratio of the thermal conductivity of the porosities (voids or obstacles) to that of the continuous phase.

Predictions of the thermal conductivity of composite mixtures are generally within 15%. Laubitz (1959) suggests that the right-hand side of Eq. (2.1) be multiplied by 2 for application to powdered solids in air. This modification was based on data obtained over a wide range of temperatures, including those at which radiation heat transfer had to be considered. The complete equation Laubitz utilized included a term to account for radiative heat transfer, and the predictions fit the data only when Russell's conductivity term was multiplied by 2. Note, however, if the right-hand side of Eq. (2.1) is multiplied by 2, the limiting case for a fluid with a zero granular fraction is too large by a factor of 2.

The ratio, ν, is given by

$$\nu = \frac{k_{\text{por}}}{k_{\text{cont}}}\ , \tag{2.2}$$

where k_{por} may be identified with k_{solid} and k_{cont} identified with k_{fluid}. The equation for porosity is given as

$$p = \frac{\rho_{\text{solid}} - \rho_{\text{comp}}}{\rho_{\text{solid}} - \rho_{\text{fluid}}} \ , \tag{2.3}$$

Often the void volume fraction, ε, is given because simple measurements of the bulk density of the granular material in air gives

$$1 - \varepsilon = \frac{\rho_{\text{bulk}}}{\rho_{\text{true}}} \ , \tag{2.4}$$

where the "true" density is identified with the density of the crystalline solid. This is an approximation and is accurate only when the density of the interstitial fluid (typically air) is small compared with the density of the crystalline solid. In a solid-phase continuous system, p is identified with ε, that is $p = \varepsilon$. In systems where the fluid phase is continuous, Laubitz specifically states that p is the fractional volume of the obstacles (the solids) and must be identified as follows:

$$p = 1 - \varepsilon \ . \tag{2.5}$$

Equations (2.1), (2.2), and (2.5) thus provide the correct approximation for the thermal conductivity of the fluid-solid composite.

Another method for calculating the effective thermal conductivity of porous media is given by Krupiczka (1967):

$$\frac{k_{\text{effective}}}{k_{\text{gas}}} = \left(\frac{k_{\text{solid}}}{k_{\text{gas}}} \right)^{A + B \log\left(\frac{k_{\text{solid}}}{k_{\text{gas}}} \right)} \ , \tag{2.6}$$

where

$$A = 0.280 - 0.757(\log \varepsilon), \tag{2.7}$$

$$B = -0.057 \ . \tag{2.8}$$

The term, ε, is the void volume fraction as before. The equation is not restricted to solid gas systems, and k_{gas} may be replaced with k_{fluid}.

2.2 Available Data and Physical Properties

2.2.1 IONSIV® IE-911™

IONSIV® IE-911™ is an inorganic ion-exchange medium used for sorption of cesium from aqueous media. The active ingredient is CST. The commercial product

contains other metal oxides and proprietary materials that are used to form microchannels in the solid-phase structure and to bind the CST particles into spherical granules. Table 2.1 summarizes the composition of the IE-911™, listing the range of weight percentages of each component. CST is given as its constituent components (SiO_2 and TiO_2), and the data indicate that the concentration of CST in IE-911™ ranges from 35 to 85 wt %.

Table 2.1. Composition[a] of IONSIV® IE-911™

Component	Formula	Wt % range
Silicon dioxide	SiO_2	15–45
Titanium dioxide	TiO_2	20–40
Sodium oxide	Na_2O	5–20
Trade secret material	–	5–25
Trade secret metal oxide	–	0–25
Aluminum oxide	Al_2O_3	0–10
Copper oxide	CuO	0–2
Calcium oxide	CaO	0–2
Chromium oxide	Cr_2O_3	0–2
Magnesium oxide	MgO	0–2

[a]*Source*: UOP, 1995.

No information on the thermal conductivity of CST or IE-911™ was found in the literature. Fennelly (2000) provided a reference value of $0.05\ W/(m \cdot K)$, or $0.08\ Btu \cdot h^{-1} \cdot ft^{-1} \cdot {}^oF^{-1}$, for zeolite, which is a mechanically similar material, and indicated that the thermal conductivity of IE-911™ should be higher. Information on the pure form of some of the components is available and is summarized in Table 2.2. As indicated in the table, thermal conductivity for SiO_2 is dependent on the crystal axis through which heat flows, basically the orientation of the crystal with respect to the temperature gradient. CST is probably polycrystalline in nature; therefore, large particles would exhibit no variation in thermal conductivity with respect to orientation. Because thermal conductivity of solids is dependent on structure, values of thermal conductivity computed from a weighted average of the values for the pure constituents will not provide reliable results. It is interesting to note that the thermal conductivities of crystalline SiO_2 and TiO_2 are roughly $6.0\ W/(m \cdot K)$, while those for aluminia and magnesia are roughly $30.0\ W/(m \cdot K)$. Therefore, the average thermal conductivity of the

minor components is about 5 times greater than that of the major component (assumed to be CST).

Table 2.2. Selected properties of IONSIV® IE-911™ components[a]

Component	Molecular weight	Density (g/cm^3)	Thermal conductivity [W/(m · K)]	Temperature (°C)
SiO_2	60.08	2.19 (amorph)	5.88[b]–11.07[c]	37.8
		2.26[d] at 25°C	5.19[b]–9.34[c]	93.3
			4.50[b]–9.00[c]	148.9
TiO_2	79.88	4.17[d] (white)	6.53 (refractory)	100.0
			5.54[b]–9.69[c]	37.8
			5.54[b]–8.30[c]	93.3
			5.54[b]–7.61[c]	148.9
Na_2O	61.98	2.27		
Al_2O_3	101.96	3.965[d] at 25°C	30.3 (refractory)	100.0
			32.35[b]–34.95[c]	37.8
			25.95[b]–27.68[c]	93.3
			22.32[b]–24.22[c]	148.9
CuO	79.55	6.3 – 6.49		
CaO	56.08	3.25 – 3.38[d]		
Cr_2O_3	151.99	5.21[d]		
MgO	40.30	3.58[d] at 25°C	36.0 (refractory)	100.0
			36.7	37.8
			31.8	93.3
			27.7	148.9

[a]*Source*: Weast, 1989, pp. D-40, E-7. Temperatures in the right-most column are associated with the values of thermal conductivity.

[b]Lower value in range is that measured along "a axis" of crystal.

[c]Upper value in range is that measured along "c axis" of crystal.

[d]Crystalline.

Because IE-911™ is a granular solid, bulk quantities of the material contain a significant volume fraction of void space. Welch et al. (2000) report the following values for the material:

bulk density = 65 lb/ft^3 (1.041 g/cm^3), and

void fraction = 0.35.

Under the assumption that the latter value refers to the total void fraction, application of Eq. (2.4) would indicate a solid density of 100 lb/ft^3 (1.602 g/cm^3), which seems low and could indicate void fractions greater than 0.35. The particle density of CST powder is reported by Miller and Brown (1997) to be ~2.9 g/cm^3, with a bulk density of 0.85 g/cm^3. These latter data indicate a total void fraction of 0.71 for the powder but do not give information pertaining to the bulk properties of IE-911™, an engineered form of CST.

2.2.2 Air and Water Vapor

Air is the gas of primary concern in the measurement of the thermal conductivity of dry CST. The thermal conductivity of dry air is available in standard references and is given in Table 2.3. Because ambient air contains a small fraction of water vapor, the thermal conductivity of water vapor is also listed in the table. The thermal conductivity of water vapor is about 60% that of dry air. At room temperature (~25°C) and a relative humidity of 60%, the volume fraction of water vapor in air is 0.019; therefore, the thermal conductivity is not significantly different from that of dry air.

Table 2.3. Thermal conductivity of dry air and water vapor[a]

	Thermal conductivity [W/(m · K)]	
Temperature (°C)	Air	Water Vapor
−17.8	0.02269	0.01452
−6.7	0.02353	0.01539
4.4	0.02440	0.01625
15.6	0.02525	0.01695
26.7	0.02602	0.01781
37.8	0.02687	0.01867
48.9	0.02763	0.01954
93.3		0.02300

[a]*Source*: Weast, 1989, p. E-3.

For most gases, the derivative of thermal conductivity with respect to temperature lies between 4.2×10^{-5} and 12.5×10^{-5} W/(m · K) over a temperature range of 30 to 200°C (Perry and Chilton, 1973). The data in Table 2.3 were correlated to a linear function of temperature,

$$k = b_0 + b_1 T , \qquad (2.9)$$

where

k = thermal conductivity, W/(m · K);

T = temperature, °C;

b_i = adjustable constants of the model.

The results for dry air are

$b_0 = 0.024042$,

$b_1 = 7.4316 \times 10^{-5}$, and

$r^2 = 0.99966$,

where r^2 is the correlation coefficient. The data and functional fit are shown in Fig. 2.1.

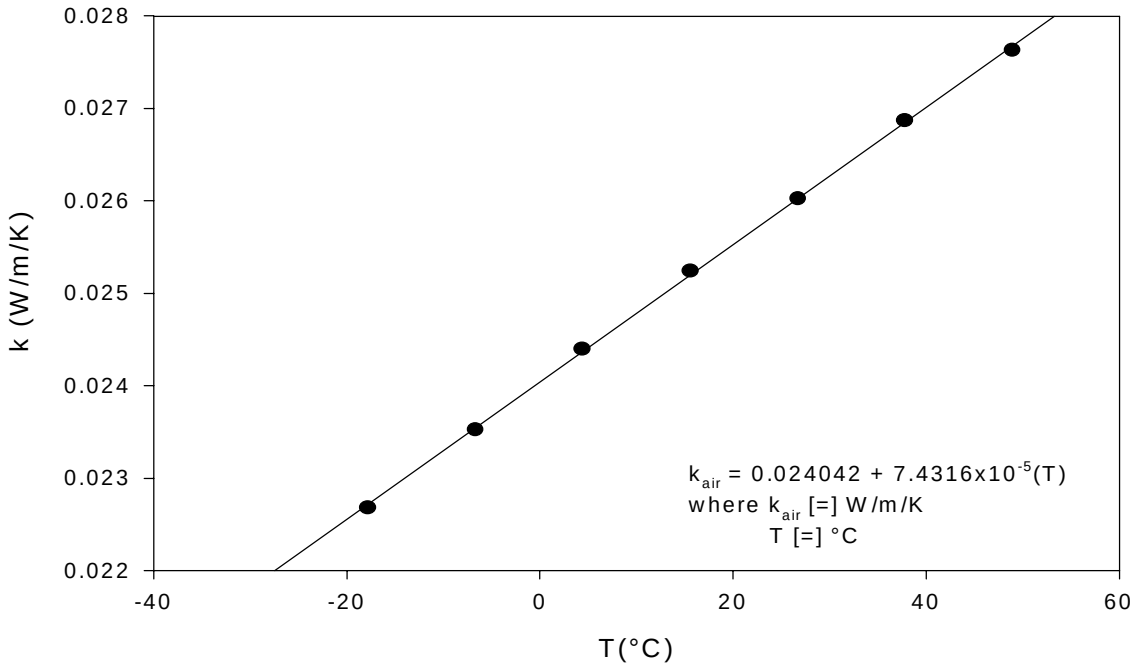

Fig. 2.1. Thermal conductivity of dry air—data compared with correlation.

At temperatures significantly above room temperature, the volume fraction of water vapor in air at saturation is significant and can dominate at the higher temperatures. The potential need for values of the thermal conductivity of water vapor encouraged correlation of the data. The results for water vapor are

$b_0 = 0.015848$,

$b_1 = 7.5899 \times 10^{-5}$, and

$r^2 = 0.99947$.

The data and functional fit are shown in Fig. 2.2. For both dry air and water vapor, the temperature coefficient falls within the range quoted by Perry and Chilton (1973).

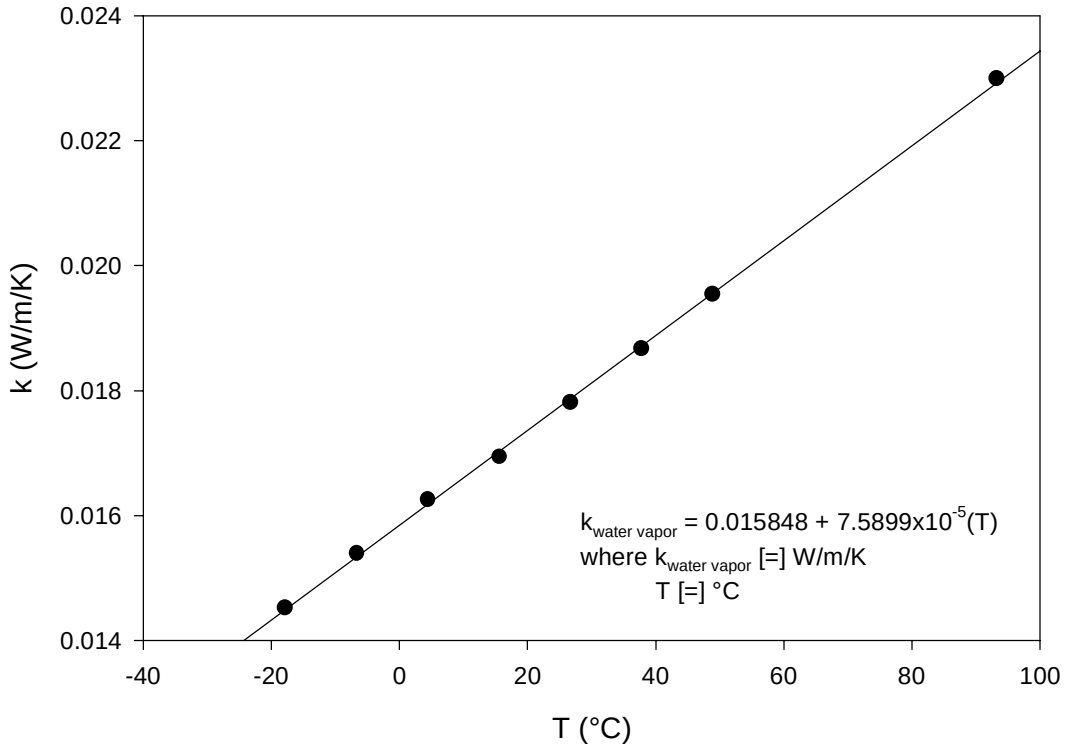

Fig. 2.2. Thermal conductivity of water vapor—data compared with correlation.

2.2.3 Water and Simulant

Reid et al. (1987) provide a method to estimate the thermal conductivity of aqueous ionic solutions over a range of temperatures. The algorithm requires values for the thermal conductivity of water, which are provided in Table 2.4. The data show that the conductivity rises to a maximum near the normal boiling point and then decreases with increasing temperature. This suggests the data may be modeled with a parabolic function,

$$k = b_0 + b_1 T + b_2 T^2 . \qquad (2.10)$$

Table 2.4. Thermal conductivity of liquid water[a]

Temperature (°C)	Thermal conductivity [W/(m · K)]
−3	0.5548
7	0.5740
27	0.6092
47	0.6368
67	0.6590
97	0.6799
107	0.6841
157	0.6812
197	0.6611
247	0.6121
297	0.5389
347	0.4201

[a]*Source*: Weast, 1989, p. E-6.

The data of interest in Table 2.4 lie between −3°C and 97°C; these were fit to Eq. (2.10) with the following result:

$b_0 = 0.56075$,

$b_1 = 1.9947 \times 10^{-3}$,

$b_2 = -7.9003 \times 10^{-6}$, and

$r^2 = 0.99998$.

Fig. 2.3 illustrates the fit of the correlation with the data.

The method described by Reid et al. (1987) to calculate the thermal conductivity of aqueous ionic solutions begins with the computation of the value at 20°C,

$$k_{\mathrm{I},\,20°\mathrm{C}} = k_{\mathrm{H_2O},\,20°\mathrm{C}} + \sum \sigma_i C_i , \qquad (2.11)$$

where

$k_{\mathrm{I},\,20°\mathrm{C}}$ = thermal conductivity of the ionic solution at 20°C, W/(m · K);

$k_{\mathrm{H_2O},\,20°\mathrm{C}}$ = thermal conductivity of water at 20°C, W/(m · K);

C_i = concentration of electrolyte *i*, mol/L;

σ_i = coefficient characteristic of each ion.

Values for σ_i are given in Table 2.5 for each component of the simulant along with the concentration appropriate for the average simulant.

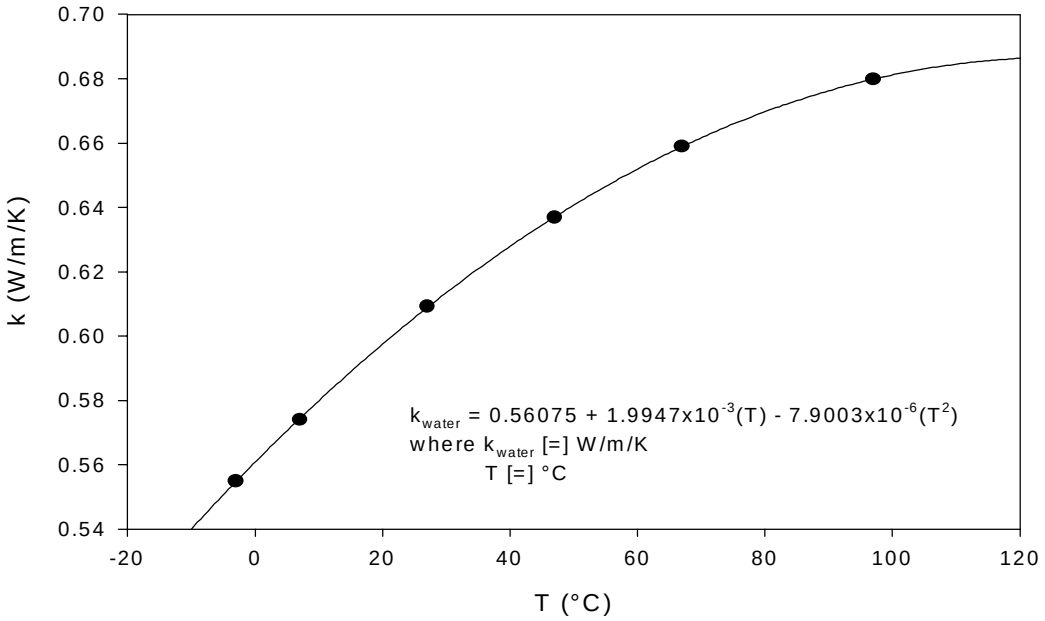

Fig. 2.3. Thermal conductivity of liquid water—data compared with correlation.

Table 2.5. Coefficients used to estimate thermal conductivity of average simulant

Component	Coef. of Eq, (2.11), σ[a]	Average simulant concn. (M)[b]
Cations		
Na^+	0	5.6
Cs^+	*c*	0.00014
K^+	-7.560×10^{-5}	0.015
Anions		
OH^-	20.934×10^{-5}	1.91
NO_3^-	-6.978×10^{-5}	2.14
NO_2^-	-4.652×10^{-5}	0.52
AlO_2^-	1.163×10^{-5} [d]	0.31
CO_3^{2-}	-7.560×10^{-5}	0.16
SO_4^{2-}	1.163×10^{-5}	0.15
Cl^-	-5.466×10^{-5}	0.025
F^-	2.0934×10^{-5}	0.032
PO_4^{3-}	-20.93×10^{-5}	0.010
$C_2O_4^{2-}$	-3.489×10^{-5}	0.008
SiO_3^{2-}	-9.300×10^{-5}	0.004
MoO_4^{2-}	*c*	0.0002

[a]*Source:* Reid et al., 1987, p. 567.

[b]*Source:* Walker, 1999.

[c]Value unavailable; zero is assumed because the concentration of this component is low.

[d]Value for aluminate assumed equivalent to that of sulfate as suggested by Bostick and Steele (1999).

The thermal conductivity of the ionic solution at other temperatures is given by

$$k_{\mathrm{I,T}} = k_{\mathrm{I,20°C}} \frac{k_{\mathrm{H_2O,T}}}{k_{\mathrm{H_2O,20°C}}}. \qquad (2.12)$$

The method is reported to estimate thermal conductivity of ionic solutions within an error of ~7%, provided that the solution is not too strong an acid or a base (concentration range not specified).

Bostick and Steele (1999) used the same algorithm to calculate the thermal conductivity of simulants at temperatures between 10 and 30°C. Their calculated value for average simulant at 20°C was 0.5922 W/(m · K). In the present work, a value of 0.5977 W/(m · K) was calculated, which is in close agreement. The thermal conductivity of water at 20°C, from Fig. 2.3, is 0.5975 W/(m · K). Thus, the thermal conductivity of the simulant is calculated to be essentially the same as that of water at 20°C. The form of Eq. (2.12) leads to the deduction that the calculated thermal conductivity of the simulant is nearly equivalent to that of water at other temperatures. Predicted values of the thermal conductivity of average simulant are shown in Table 2.6 for temperatures ranging from 0 to 100 in 10°C increments. The thermal conductivity of water is included for comparison.

Table 2.6. Predicted thermal conductivity of average simulant compared with that of water

	Thermal conductivity [W/(m · K)]	
Temperature (°C)	Water	Simulant
0.0	0.5608	0.5610
10.0	0.5799	0.5801
20.0	0.5975	0.5977
30.0	0.6135	0.6137
40.0	0.6279	0.6281
50.0	0.6407	0.6410
60.0	0.6520	0.6522
70.0	0.6617	0.6619
80.0	0.6698	0.6700
90.0	0.6763	0.6765
100.0	0.6812	0.6815

A measured thermal conductivity of 0.68 W/(m · K) for average simulant solution at 19°C was reported by Bostick and Steele (1999). This value is ~14% higher than the predicted value and exceeds the variation expected of the model. It is likely that the base concentration in the simulant is outside the upper limit for the model. Convective heating caused by the sensor during measurement may have also contributed to the error.

2.3 Initial Estimates

The volume fraction of void spaces in the granulated solids will be, under normal circumstances, filled with a fluid. Typical fluids include salt waste solution, water, and air. The thermal conductivity of these fluids is given in Table 2.7.

Table 2.7. Thermal conductivity of selected fluids

Fluid	Thermal conductivity [W/(m · K)]	Temperature (°C)	Reference
Simulant (liquid)	0.68	19	Bostick and Steele, 1999
Water (liquid)	0.592	20	Weast, 1989, p. E-11
Air (gas)	2.553×10^{-2}	20	Fig. 2.1, this report

An order-of-magnitude estimate of the thermal conductivity of the IE-911™ solid is 10.0 W/(m · K). Comparing with the data in Table 2.7,

$$k_{\text{solid}} \approx 10 k_{\text{simulant}} \tag{2.13}$$

and

$$k_{\text{solid}} \approx 250 k_{\text{air}} . \tag{2.14}$$

This would indicate that the thermal conductivity of the solid-fluid composite is depressed relative to that of an individual solid particle. The thermal conductivity of the solid-fluid composite is predicted by straightforward application of Eq. (2.1) or Eq. (2.6). To explore the effect of uncertainty associated with the estimated thermal conductivity of the solid, values 20% higher and 20% lower than the estimated value of 10.0 W/(m · K) were selected. The results are given in Tables 2.8 and 2.9.

Table 2.8 summarizes the estimated thermal conductivity of IE-911™ immersed in air, that is, a composite formed by IE-911™ and air. Effective thermal conductivities

of ~ 0.2 W/(m · K) are calculated by the Russell method. These results indicate that a variation of ±20% in k_{solid} causes a variation of only ±0.5% in the thermal conductivity of the composite calculated by the method of Russell. Values calculated by the Krupiczka method are about twice those calculated by the Russell method. This leads to the question of whether the Russell equation including the Laubitz correction would be more correct in this application. The same variation in k_{solid} results in a variation of 7% in the thermal conductivity of the composite calculated by the method of Krupiczka.

Table 2.8. Estimated thermal conductivity [W/(m · K)] of IONSIV® IE-911™ immersed in air at 20°C[a]

Value of k_{solid} (assumed)	Calculated value of $k_{composite}$	
	Russell method	Krupiczka method
8	0.1858	0.4095
10	0.1868	0.4413
12	0.1874	0.4683

[a] $\varepsilon = 0.35$, $k_{air} = 2.553 \times 10^{-2}$ W/(m · K).

Table 2.9 summarizes the estimated thermal conductivity of IE-911™ immersed in salt waste simulant, that is, a composite formed by IE-911™ and simulant. Effective thermal conductivities of ~ 3.0 W/(m · K) are calculated. These results indicate that a variation of ±20% in k_{solid} causes a variation of ±8% in the thermal conductivity of the composite calculated by the method of Russell. The same variation in k_{solid} results in a variation of 10% in the thermal conductivity of the composite calculated by the method of Krupiczka. It is noteworthy that the estimate made by the Russell method compares closely with that obtained through the Krupiczka method. This indicates that the Laubitz correction to the Russell equation, in this instance, is not necessary.

Table 2.9. Estimated thermal conductivity [W/(m · K)] of IONSIV® IE-911™ immersed in simulant at 20°C[a]

Value of k_{solid} (assumed)	Calculated value of $k_{composite}$	
	Russell method	Krupiczka method
8	2.967	2.732
10	3.230	3.053
12	3.435	3.336

[a] $\varepsilon = 0.35$, $k_{simulant} = 0.68$ W/(m · K).

3. EXPERIMENTAL APPARATUS AND REAGENTS

3.1 Equipment

Thermal conductivity of air-dried CST and a mixture of CST with supernatant waste simulant was measured using the transient plane source method. The instrument used was a hot disk thermal constants analyzer, the same equipment that was previously used to measure the thermal conductivity of waste simulant (Bostick and Steele, 1999). A Kapton polyamide sensor, shown in Fig. 3.1, was placed in the sample. Sample sizes

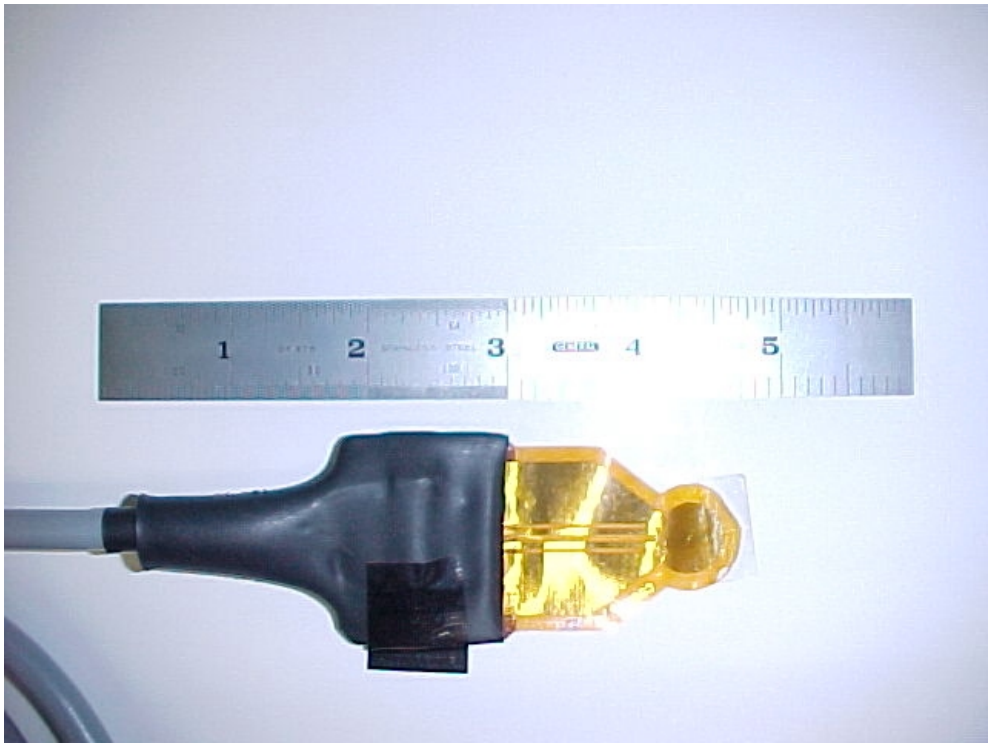

Fig. 3.1. Sensor used for measurement of thermal conductivity.

ranged from 200 to 300 mL. The sample (with the sensor) was placed in a temperature-controlled oven, as shown in Fig. 3.2. The sample was heated to the temperature at which the thermal conductivity was to be measured. The analyzer provides a step increase in current to the heating elements within the sensor (duration of ~80 s) and calculates the thermal conductivity from the resulting temperature-vs-time data. Up to five measurements were made, with relaxation times between measurements of ~30 min.

Fig. 3.2. Controlled-temperature oven with sample beaker inside.

3.2 Materials

3.2.1 Supernatant Simulant

Supernatant simulant was prepared using a recipe supplied by SRS (Walker, 1999) and is similar to solutions used in previous tests at Oak Ridge National Laboratory (ORNL). The concentrations of salts in the average simulant are shown in Table 3.1. Deionized water was used to prepare the solution. Chemicals used in the preparation of the supernatant were of reagent grade, purchased from commercial sources.

Table 3.1. SRS average supernatant waste composition[a]

Component	Average concn. (*M*)
Na^+	5.6
Cs^+	0.00014
K^+	0.015
OH^-	1.91
NO_3^-	2.14
NO_2^-	0.52
AlO_2^-	0.31
CO_3^{2-}	0.16
SO_4^{2-}	0.15
Cl^-	0.025
F^-	0.032
PO_4^{3-}	0.010
$C_2O_4^{2-}$	0.008
SiO_3^{2-}	0.004
MoO_4^{2-}	0.0002

[a]*Source:* Walker, 1999.

3.2.2 Granulated CST

The CST used for these tests was the commercial, granular form of the sorbent, IONSIV® IE-911™ (UOP Molecular Sieves, Mt. Laurel, New Jersey). All tests were made with material from lot no. 999098810005. The as-received CST was pretreated using the steps recommended by the manufacturer and agreed upon by ORNL and SRS. This includes treatment with dilute sodium hydroxide to adjust the pH to ~13, backwashing with water to remove fines, draining the water from the solids, treatment with 1.9 *M* sodium hydroxide solution, and then draining the solids and air drying for 3 days.

4. RESULTS AND DISCUSSION

4.1 Density and Void Fraction of IE-911™

Simple experiments were performed to obtain the void fraction of IE-911™. The CST was slow poured into a 25-mL graduated cylinder to the full mark. Weighing the cylinder before and after filling with CST provided the mass of a 25-mL volume of the granulated material. The density of air-dried material was calculated from those data. Ethyl alcohol was added to displace the air. Alcohol was used because of its propensity to rapidly penetrate porous media. Direct addition of alcohol was problematic because air could become trapped in the interstitial voids. A more effective procedure was to remove the CST to a secondary container, place alcohol in the graduated cylinder, and then pour the CST slowly back into the cylinder as additional alcohol was incrementally added. As the CST fell through the alcohol, very fine bubbles were observed to rise from the submerged bed. These bubbles could have originated from air released from inside individual particles as the alcohol penetrated the material. The CST would not settle to the 25-mL mark unless the container was tapped, and settling still remained difficult. CST is known to swell in aqueous simulant solution (Bostick and Steele, 1999). Thus, swelling of the CST may have occurred, or simple reproduction of the packing may have been the problem. Weight measurements of the alcohol, along with its density, provided the void volume. Possible changes in the volume of the alcohol caused by dissolution of salts associated with the CST (e.g., sodium hydroxide) were ignored.

The results are summarized in Table 4.1 In spite of the difficulties described above, the data are believed to be reliable. The bulk density of air-dried IE-911™ was 1.168 g/mL (±0.037 g/mL). Because additional water can be driven from the CST by heating, this value of density is slightly higher than that of bone-dry material. The void fraction was estimated at 0.432 (±0.012), which is greater than the value of 0.35 discussed in Sect. 2.2.1 and has a substantial impact on estimations of the thermal conductivity of a composite mixture. The indicated density of the solid material, correcting for the void fraction, is 2.06 g/cm^3, which is close to that of amorphous silicon dioxide.

Table 4.1. Density and void fraction of air-dried IE-911™ (lot no. 999098810005)[a]

		Interstitial fluid added		Calculated	
Trial	CST (g)	Ethanol (g)	Ethanol (mL)[b]	Density (g/cm^3)	Void fract.
1	28.644	8.334	10.58	1.146	0.423
2	28.260	8.324	10.56	1.130	0.422
3	29.684	8.523	10.82	1.187	0.433
4	30.246	8.761	11.19	1.210	0.448
			Avg.	1.168	0.432
			Std. dev.	0.037	0.012

[a]Measurements made in a 25-mL graduated cylinder.

[b]Measured density of ethanol was 0.788 g/mL, which compares closely with the value of 0.787 g/mL at 23°C listed in Weast, 1989.

4.2 Thermal Conductivity of Dry CST

4.2.1 Initial Tests

The thermal conductivity of air-dried IE-911™ was measured using the equipment described in Sect. 3. The CST was slow poured (i.e., without agitation or vibration) around the sensor while it was suspended in the test beaker. Up to five measurement trials were made at each test temperature to obtain thermal conductivity. The results are shown in Table 4.2. Data in the table are shown in the order collected. In addition, the data are grouped to facilitate discussion.

In the first test sequence (labeled "test on fresh sample A" in Table 4.2), the measured thermal conductivity initially increased with rising temperature, reached a maximum, and then decreased with increasing temperature. Measurements made as the sample was cooled from the highest temperature (120°C) did not return along the same conductivity-temperature curve. The results of the test sequence are shown in Fig. 4.1. Hysteresis in the measured thermal conductivity was thought to be caused by absorbed water or waters of hydration. The vapor pressure of water for this system is strongly dependent on temperature. Latent heat effects would inflate measured values of thermal conductivity. For example, vaporization of water near the probe, coupled with diffusive transport of water vapor to a cooler region of the test matrix where the water vapor could condense, represents a heat transfer process operating coincidentally with conduction.

Table 4.2. Thermal conductivity of air-dried CST

	Measured thermal conductivity [W/(m · K)]						
Temp. (°C)	1	2	3	4	5	Avg.	Std. dev.
Test on fresh sample A							
20.0	0.2631	0.2570	0.2638	0.2548	0.2506	0.2579	0.0056
50.0	0.4739	0.4479	0.4642	0.4306	0.4332	0.4500	0.0189
120.0	0.1431	0.1543	0.1564	0.1432	0.1501	0.1494	0.0062
104.7	0.1506	0.1567	0.1481	0.1491	0.1437	0.1496	0.0047
59.2	0.1209	0.1192	0.1316	0.1289	0.1345	0.1270	0.0067
25.0	0.1155	0.1106	0.1117	0.1096	0.1120	0.1119	0.0022
21.4	0.1087	0.1110				0.1099	0.0016
Test on fresh sample B							
22.0	0.2824	0.2732	0.2766	0.2880	0.2673	0.2775	0.0080
Retest on sample A after standing at room conditions for 3 days							
21.0	0.1297	0.1240	0.1314	0.1306	0.1288	0.1289	0.0029
50.0	0.1361	0.1394	0.1336	0.1345	0.1456	0.1378	0.0049

Further tests were made to check the hypothesis that moisture caused the hysteresis. A measurement was made on a fresh sample of the air-dried powder (labeled "test on fresh sample B" in Table 4.2). The thermal conductivity of this sample was high, as would be expected from the increasing-temperature curve of Fig. 4.1. The original sample was retested after standing at room conditions for 3 days (labeled "retest on sample A after standing at room conditions for 3 days" in Table 4.2). The data show that the thermal conductivity increased but not to the initial values. Although the former level of moisture was probably not restored in that short period of time, the increase in thermal conductivity was indicative that moisture content affected the apparent thermal conductivity.

The nearly linear thermal conductivity-temperature curve obtained on CST that had been heated above 100°C was thought to indicate that the powder was dry and free of water-related latent heat effects. However, it seemed clear that planned tests on wetted material (i.e., CST soaked in simulant and then simply drained of the bulk liquid) would be marred by latent heat effects.

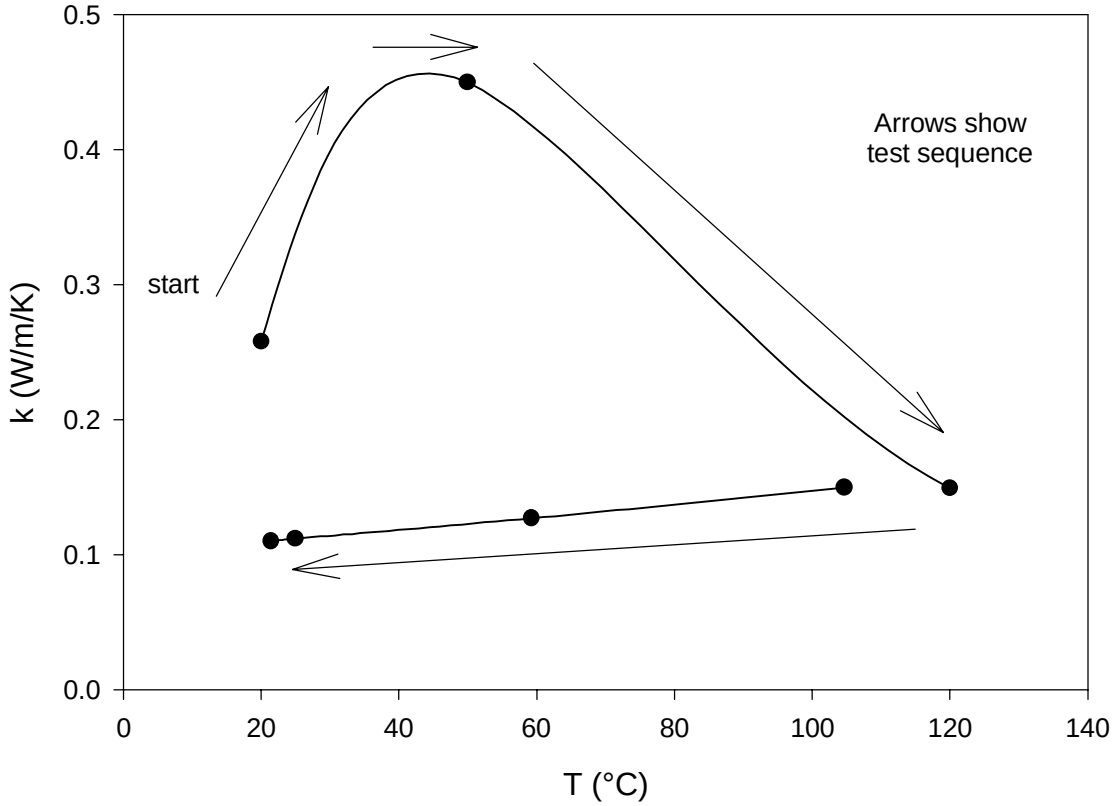

Fig. 4.1. Hysteresis in thermal conductivity of air-dried CST.

4.2.2 Desiccation of CST IE-911™

Concerns that high-temperature drying would alter the physical structure, and subsequently thermal conductivity, led to consideration of vacuum drying or desiccation. Desiccation was selected because materials and equipment were readily available. Two samples were placed in a Labconco vacuum oven (without heating) in the presence of a large excess of ascarite. The samples were periodically weighed, with results as shown in Table 4.3. Weight loss is evident, and when the samples were returned to the room environment, weight gain was evident. Because reabsorption of moisture was slow, desiccated CST was judged acceptable for thermal conductivity tests. A 1-L sample of CST was dried using the data in Table 4.3 as a guideline for drying time.

Table 4.3. Trial drying of CST by desiccation

Day	Mass (g)		Comment
	Sample 1	Sample 2	
0	10.483	10.870	Initial, air-dried sample
3	9.854	10.210	
6	9.788	9.991	
13	9.644	9.925	
17	9.416	9.742	
18	9.301	9.739	After weighing, sample placed to room environ.
20	9.583	9.928	Weight gain evident

4.2.3 Thermal Conductivity of Dried IE-911™

The thermal conductivity of desiccated IE-911™ was measured using the steps previously described. Data were obtained up to temperatures of ~130°C. Above this temperature, the polymer-type sensor was damaged. Thus, the upper limit to reliable measurements was established.

The data are shown in Table 4.4. Hysteresis between the measurements made in order of ascending temperature, compared with those in order of descending temperature, was not as evident as before. Thermal conductivity of CST obtained on samples that had been heated to >100°C and/or desiccated were presumed reliable (i.e., free of latent heat effects). Such data are summarized and annotated in Table 4.5. These data are plotted as

Table 4.4. Thermal conductivity of desiccated CST

Temp. (°C)	Measured thermal conductivity [W/(m · K)][a]						
	1	2	3	4	5	Avg.	Std. dev.
23.0	0.1207	0.1191	0.1247	0.1169	0.1233	0.1209	0.0031
55.6	0.1304	0.1327	0.1463	0.1271	0.1440	0.1361	0.0085
129.6	0.1242	0.1285	0.1324	0.1369	0.1271	0.1298	0.0049
96.6	0.1309	0.1371	0.1398	0.1293	0.1348	0.1344	0.0043
55.0	0.1293	0.1282	0.1128	0.1285	0.1161	0.1230	0.0079
23.0	0.1041	0.1131	0.1097	0.1094	0.1101	0.1093	0.0033

[a]Measured over a 2-day period with barometric pressure of 29.09 in Hg the first day and 29.08 in Hg the second day.

Table 4.5. Thermal conductivity of dried CST

Temperature (°C)	Thermal conductivity [W/(m · K)] Average	Std. dev.	Comments
21.4	0.1099	0.0016	Dried at >100°C
25.0	0.1119	0.0022	Dried at >100°C
59.2	0.1270	0.0067	Dried at >100°C
104.7	0.1496	0.0047	Dried at >100°C
120.0	0.1494	0.0062	Dried at >100°C
23.0	0.1209	0.0031	Desiccated at ~21°C
55.6	0.1361	0.0085	Desiccated at ~21°C
23.0	0.1093	0.0033	Desiccated, dried at >100°C
55.0	0.1230	0.0079	Desiccated, dried at >100°C
96.6	0.1344	0.0043	Desiccated, dried at >100°C
129.6	0.1298	0.0049	Desiccated, dried at >100°C

a scattergram in Fig. 4.2. A small difference appears to exist between CST that was only desiccated and that which was, by the nature of the experiment, dried at temperatures above 100°C. The data were correlated to a straight line by regression analysis. The correlation coefficient was 0.67 when the data set included the two points from measurements on desiccated-only CST but became 0.76 if these two points were omitted. Further omission of the one point at 129.6°C caused the correlation coefficient to become 0.96. This point could have been an outlier because of thermal damage to the sensor. In summary, the thermal conductivity of dry CST in air was correlated to a linear function [form of Eq. (2.9)] with the following results:

$$k_{\text{CST}-\text{air}} = 0.10096 + 4.0960 \times 10^{-4} T \ , \qquad (4.1)$$

where $k_{\text{CST-air}}$ = thermal conductivity of the CST-air mixture, W/(m · K); T = temperature, °C; and the correlation coefficient of $r^2 = 0.96019$.

The data are compared with the linear model in Fig. 4.3. (Note: More significant digits are included in the model parameters than are justified by the data. This practice, which permits the data to be reconstituted from the model, is done throughout this report.)

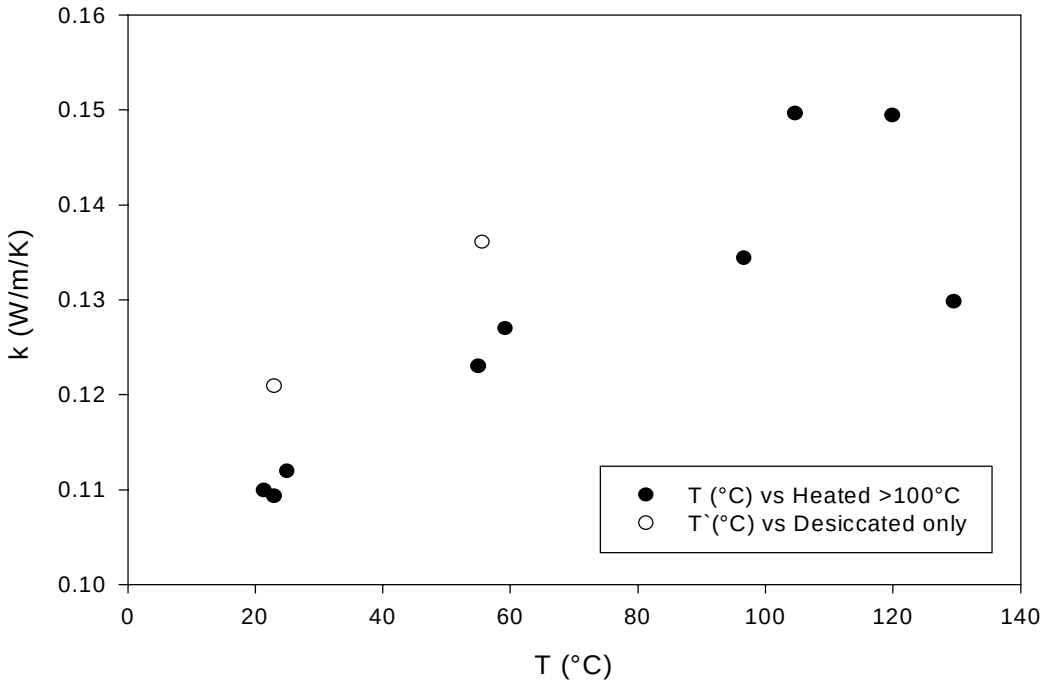

Fig. 4.2. Scattergram of thermal conductivity of dried CST versus temperature.

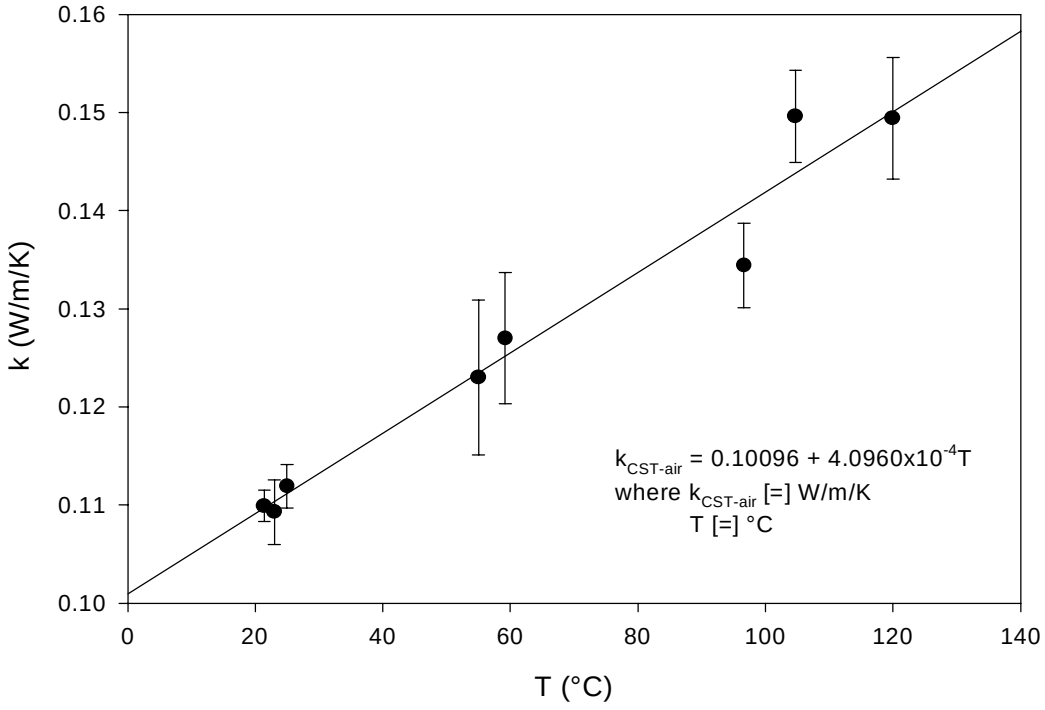

Fig. 4.3. Thermal conductivity of dry CST-air composite mixture.

4.2.4 Thermal Conductivity of Solid Particles

The effective thermal conductivity of the CST-air mixture is the property that was measured. Methods developed by Russell (1935) and Krupiczka (1967) are typically used to estimate thermal conductivities of mixtures (see Sect. 2.1). Conceptually, the methods may be used to deconvolute the solid-phase conductivity from measurements of the mixture when the thermal conductivity of the fluid is known independently. Knowledge of the void fraction of the solids is also required. The thermal conductivity of the solid-phase CST was estimated from the data given in Table 4.5 by iterative solution of Eqs. (2.1) and (2.6). In both cases, the thermal conductivity of air was calculated with the equation shown in Fig. 2.1, with the void fraction fixed at 0.432. The results are shown in Table 4.6.

Table 4.6. Calculated thermal conductivity of IE-911™ solid phase[a]

	Calculated thermal conductivity [W/(m · K)]	
Temperature (°C)	Russell method [b]	Krupiczka method [c]
21.4	0.4924	0.1535
25.0	0.5127	0.1568
59.2	0.6460	0.1804
104.7	0.9253	0.2172
120.0	0.8008	0.2135
23.0	0.4758	0.1520
55.0	0.5845	0.1732
96.6	0.6092	0.1880

[a]Void fraction assumed constant at 0.432.
[b]Data correlate with $k_{solids} = 0.41219 + 3.4644 \times 10^{-3} T$, T in °C, $r^2 = 0.75$.
[c]Data correlate with $k_{solids} = 0.13968 + 6.2800 \times 10^{-4} T$, T in °C, $r^2 = 0.93$.

In both models, the calculated thermal conductivity of the solid phase was lower than expected based on the conductivity of the CST components (Table 2.2). The shape of the Russell function was plotted as in Fig. 4.4 in an effort to explain this finding. Above values of about 1 to 2 W/(m · K), increasing the value of the thermal conductivity of the solid phase has little effect on the thermal conductivity of the composite mixture. This feature offers advantages in estimating the thermal conductivity of mixtures from properties of the constituents. However, for a reciprocal calculation, it means that small

errors in the measured value of a mixture could lead to large errors in extracted values for one of the constituents. Another interesting property of the function is that at high thermal conductivities of the solid phase, the thermal conductivity of a mixture depends strongly on the void fraction. However, at low conductivity of the solid (values approaching that of the fluid phase), the void fraction has little effect.

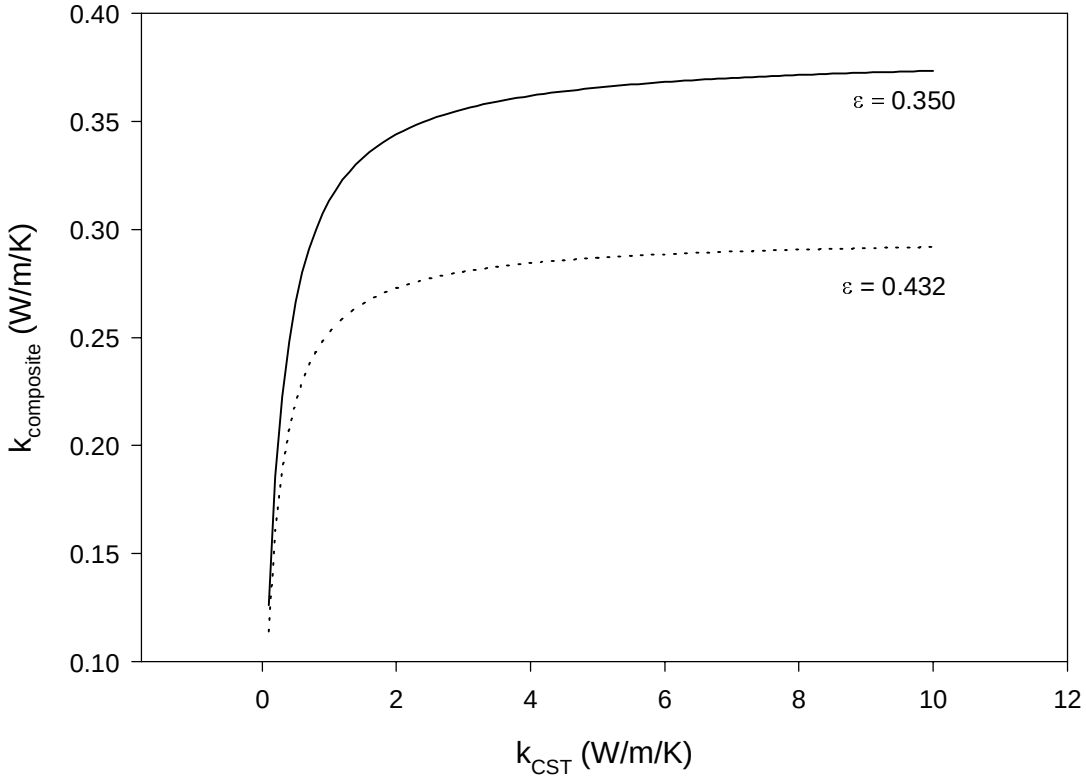

Fig. 4.4. Calculated thermal conductivity of a CST-air mixture at 25°C; dependence on void fraction and conductivity of the solid phase.

In spite of these difficulties, the calculated thermal conductivity of the solid phase obtained by deconvolution of the experimental data exhibited order (i.e., results were not random). The data were correlated by linear functions of temperature and are given in the footnotes to Table 4.6. Fig. 4.5 illustrates the thermal conductivities isolated by both the Russell and Krupiczka models. The Russell equation gives consistently higher values of thermal conductivity of the solid, that are significantly higher than that for the air-solids composite. Those values calculated from the Krupiczka method are not much

higher than that of the composite. The temperature dependence of the data reduced by the Krupiczka model better fits a linear function than does that for data reduced by the Russell equation. However, the more-linear results derived by the Krupiczka model are thought to be caused by the collapse of the reduced data to a near-constant value (i.e., the temperature dependence is masked). The Russell equation and the results for the thermal conductivity of the solids derived with it will be used for estimations of the thermal conductivity of CST-simulant mixtures. The thermal conductivity of the solids is given by

$$k_{\text{solids}} = 0.41219 + 3.4644 \times 10^{-3} T \,. \tag{4.2}$$

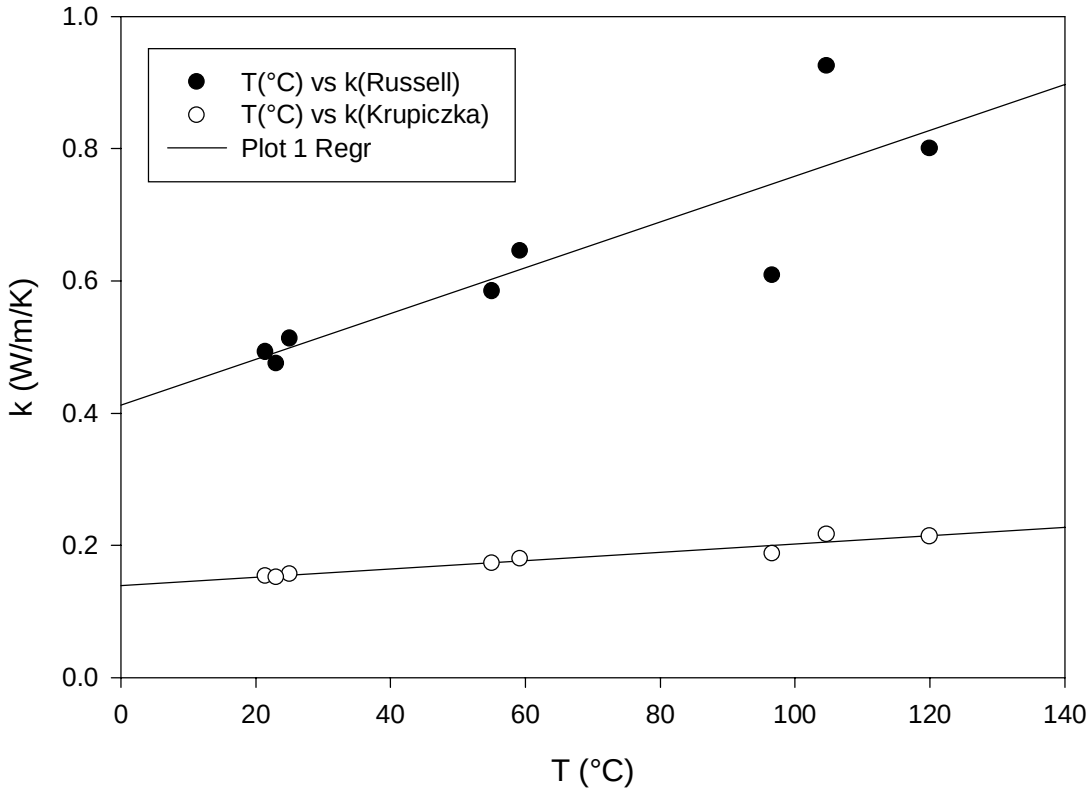

Fig. 4.5. Thermal conductivity of the CST solid phase as isolated by the Russell and Krupiczka equations.

4.3 Thermal Conductivity of CST-Simulant Mixture

The thermal conductivity of IE-911™ immersed in average simulant was measured. Initially there were difficulties with air bubbles getting trapped in the wet sand-like sample. The samples were also found to dry out quickly. These problems were solved by directing close attention to placing the sensor into the CST and adding the simulant. Leaving a ¼- to ½-in. layer of excess simulant on top of the solids bed provided a visible indicator that the sample remained wetted. The rapid drying of the sample prevented reliable measurements of thermal conductivity above ~65°C. The data are shown in Table 4.7.

Table 4.7. Thermal conductivity of CST-simulant mixture

	Measured thermal conductivity [W/(m · K)]						
Temp. (°C)	1	2	3	4	5	Avg.	Std. dev.
First sample, little excess simulant layer							
21.0[a]	0.1985	0.1884	0.2058			0.1976	0.0087
21.0	0.6067	0.6064	0.6488	0.6240	0.6665	0.6305	0.0266
50.5	0.7134	0.7263	0.7290	0.7107	0.6901	0.7139	0.0155
Second sample, with excess simulant layer							
23.0[a]	0.1041	0.1131	0.1097	0.1094	0.1101	0.1093	0.0033
27.0	0.6513	0.6579	0.7088	0.6204	0.6363	0.6549	0.0334
65.0	0.6930	0.6846	0.6993	0.6984	0.6571	0.6865	0.0174

[a]Measurement made on dried CST, as a reference, before simulant was added.

4.3.1 Comparison of Data with Calculation

The thermal conductivity of the solid-phase IE-911™ material was previously determined [see Eq. (4.2)], and that of the simulant may also be calculated (see methods in Sect. 2.2.3). The void fraction of the solids was assumed to be the same for CST-air and CST-simulant mixtures, that is, 0.432. With this information, Eq. (2.1) can be used to predict the thermal conductivity of the CST-simulant mixture. The data from Table 4.7 are compared with the calculated results in Fig. 4.6. The data points are slightly higher than predicted. The predicted values could be low because the theoretical thermal conductivity of the simulant is low.

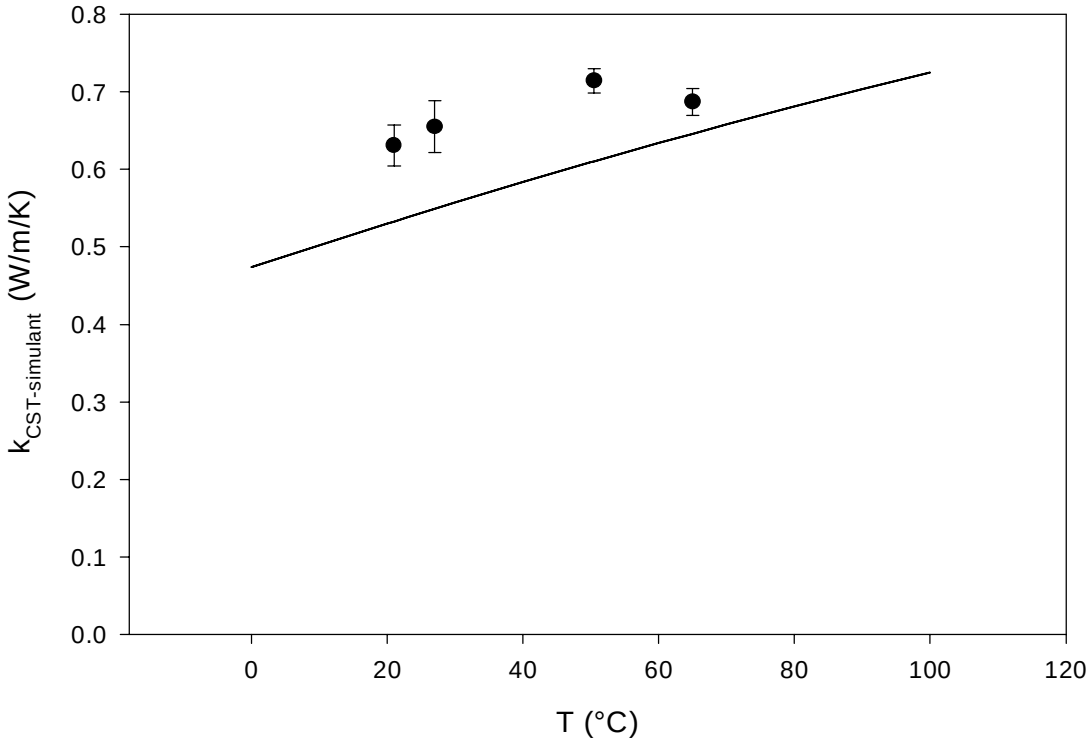

Fig. 4.6. Comparison of the predicted thermal conductivity of a CST-simulant mixture with experimental data.

4.3.2 Deconvolution of Thermal Conductivity of Simulant from Experimental Data

The thermal conductivity of the simulant can be extracted from the measured thermal conductivity of the solids-simulant mixture. Physically, the presence of the solid particles tends to attenuate natural convection in the fluid and, in concept, provides the potential to yield a value of the thermal conductivity of the fluid that is not affected by convective effects. With values of the thermal conductivity of the solid phase calculated by Eq. (4.2) and a fixed value of the void fraction of 0.432, the thermal conductivity of the simulant was calculated by iterative solution of the Russell equation. Results are given in Table 4.8. The values of thermal conductivity of the simulant extracted from the experimental values for the CST-simulant mixture are of the proper order of magnitude. However, the values are larger than would be expected based on the value of

0.68 W/(m · K) measured by Bostick and Steele (1999). In addition, the decrease in thermal conductivity with increasing temperature is opposite to expectations. Based on these findings, the values shown in Table 4.8 do not contribute additional reliable data on the thermal conductivity of the simulant.

Table 4.8. Thermal conductivity of average simulant obtained by deconvolution of data for a CST-simulant mixture

Temperature (°C)	Thermal conductivity [W/(m · K)]
21.0	0.8472
27.0	0.8766
50.5	0.8979
65.0	0.7539

5. CONCLUSIONS AND RECOMMENDATIONS

5.1 Conclusions

The thermal conductivity of CST-air and CST–average simulant mixtures were measured over temperature ranges of 20 to 130°C and 23 to 65°C, respectively. The void fraction of granulated CST was also measured because this parameter is important in predicting the thermal conductivity of two-phase mixtures from the conductivities of the component parts.

The thermal conductivity of CST-air mixtures increased linearly with increasing temperature. Methods available in the literature to estimate the thermal conductivity of two-phase mixtures from those of the components were used to back-calculate the thermal conductivity of the solid phase. The conductivity of the solid phase also varied nearly linearly with temperature.

A limited number of measurements of the thermal conductivity of CST-simulant mixtures were made. The tendency of water to evaporate rapidly from the mixture, resulting in crystallization of the salts, limited the upper temperature at which thermal conductivity could be measured. Literature methods were available to estimate the thermal conductivity of aqueous ionic solutions. Results of these calculations were combined with the thermal conductivity of the solid phase to estimate the conductivity of CST–average simulant mixtures. The experimentally measured thermal conductivity of the mixture compared reasonably well with the calculations.

Latent heat effects associated with adsorbed water or waters of hydration were observed. The information made it clear that measurements of thermal conductivity of wet CST (i.e., immersed and then drained of the bulk liquid) would be compromised.

5.2 Recommendations

It is recommended that the thermal conductivity of the simulant solutions be measured over a range of temperatures. Additional data are also needed on the thermal conductivity of CST-simulant mixtures under similar conditions.

REFERENCES

D. A. Bostick and W. V. Steele, *Thermal and Physical Property Determinations for Ionsiv® IE-911™ Crystalline Silicotitanate and Savannah River Site Waste Simulant Solutions*, ORNL/TM-1999/133, Lockheed Martin Energy Research Corp., Oak Ridge National Laboratory, August 1999.

D. Fennelly, UOP Molecular Sieves, Inc., personal communication to B. B. Spencer, Oak Ridge National Laboratory, February 4, 2000.

R. A. Jacobs, *Technical Task Request: Alternate Column Configuration and Heat Transfer–Gas Disengagement and Heat Transfer Measurements*, HLW-SDT-TTR-99-32, Westinghouse Savannah River Company, December 20, 1999.

R. Krupiczka, "Analysis of Thermal Conductivity in Granular Materials," *Int. Chem. Eng.* **7**(1), 122–144 (1967).

M. J. Laubitz, "Thermal Conductivity of Powders," *Can. J. Phys.* **37**, 798–808 (1959).

J. E. Miller and N. E. Brown, *Development and Properties of Crystalline Silicotitanate (CST) Ion Exchangers for Radioactive Waste Applications*, SAND97-0771, Sandia Corporation, Sandia National Laboratories, April 1997.

R. H. Perry and C. H. Chilton, *Chemical Engineer's Handbook*, 5th ed., McGraw-Hill Book Company, New York, 1973.

R. C. Reid, J. M. Prausnitz, and B. E. Poling, *The Properties of Gases and Liquids*, 4th ed., McGraw-Hill Inc., New York, 1987.

H. W. Russell, "Principles of Heat Flow in Porous Insulators," *J. Am. Ceram. Soc.* **18**, 1–5 (1935).

B. B. Spencer, *Technical Task Plan for Engineering Trade Studies and Support: Alternate Column Configuration and Gas Disengagement Equipment*, ORNL/CF-99/68, Rev. 0, Lockheed Martin Energy Research Corp., Oak Ridge National Laboratory, January 2000.

UOP, Material Safety Data Sheet, UOP Molecular Sieves, Inc., Des Plaines, Illinois, 1995.

D. D. Walker, *Preparation of Simulated Waste Solutions*, WSRC-TR-99-00116, Westinghouse Savannah River Company, March 12, 1999.

R. C. Weast, ed., *CRC Handbook of Chemistry and Physics*, 70th ed., CRC Press, Inc., Boca Raton, Florida, 1989.

T. D. Welch, K. K. Anderson, D. A. Bostick, T. A. Dillow, M. W. Geeting, R. D. Hunt, R. Lenarduzzi, A. J. Mattus, P. A. Taylor, and W. R. Wilmarth, *Hydraulic Performance and Gas Behavior of a Tall Crystalline Silicotitinate Ion-Exchange Column*, ORNL/TM-1999/103, Lockheed Martin Energy Research Corp., Oak Ridge National Laboratory, February 2000.

INTERNAL DISTRIBUTION

1. K. K. Anderson
2. D. A. Bostick
3. R. D. Hunt
4. R. T. Jubin
5. T. E. Kent
6. D. D. Lee
7. A. J. Mattus
8. C. P. McGinnis
9. L. E. McNeese
10. K. E. Plummer
11. S. M. Robinson
12-16. B. B. Spencer
17. H. Wang
18. T. D. Welch
19. ORNL Central Research Library
20. Laboratory Records, RC
21. Laboratory Records, OSTI

EXTERNAL DISTRIBUTION

22. Joe T. Carter, Westinghouse Savannah River Company, P.O. Box 616, 704-3N, Room S151, Aiken, SC 29808
23. Dennis Fennelly, UOP LLC, 307 Fellowship Road, Suite 207, Mt. Laurel, NJ 08054
24. Samuel D. Fink, Westinghouse Savannah River Company, P.O. Box 616, 773-A, Room B112, Aiken, SC 29808
25. Mark W. Geeting, Westinghouse Savannah River Company, P.O. Box 616, 704-196N, Room S411, Aiken, SC 29808
26. Roger L. Gilchrist, Pacific Northwest National Laboratory, P.O. Box 999, MS:K9-91, Richland, WA 99352
27. T. S. Gutmann, U.S. Department of Energy, Savannah River Operations Office, P.O. Box A, Aiken, SC 29802
28. J. O. Honeyman, Lockheed Martin Hanford Corporation, P.O. Box 1500, MS: G3-21, Richland, WA 99352
29. R. A. Jacobs, Westinghouse Savannah River Company, P.O. Box 616, 704-3N, Room S252, Aiken, SC 29808
30. Jim Jewett, Numatec Hanford Corporation, P.O. Box 1970, Richland, WA 99352
31. Robert T. Jones, Westinghouse Savannah River Company, P.O. Box 616, 704-3N, Room S122, Aiken, SC 29808.
32. R. A. Kirkbride, Numatec Hanford Corporation, P.O. Box 1970, MS: H5-27, Richland, WA 99352
33. C. S. Louie, U.S. Department of Energy, Richland Operations Office, P.O. Box 550, MSIN: B4-55, Richland, WA 99352
34. James W. McCullough, U.S. Department of Energy, Savannah River Operations Office, P.O. Box A, Building 704-3N, Room S101, Aiken, SC 29802
35. J. P. Morin, Westinghouse Savannah River Company, P.O. Box 616, Savannah River Technology Center, 703-H, Aiken, SC 29808
36. Lynn Nelson, Westinghouse Savannah River Company, P.O. Box 616, 773-A, Room-B-112, Aiken, SC 29808
37. J. R. Noble-Dial, U.S. Department of Energy, Oak Ridge Operations Office, P.O. Box 2001, Oak Ridge, TN 37831-8620

38. Arlin Olson, Idaho National Engineering and Environmental Laboratory, Building 637, MS-5218, Idaho Falls, ID 83415-5218
39. L. M. Papouchado, Westinghouse Savannah River Company, P.O. Box 616, 773-A, Room A-263, Aiken, SC 29808
40. Reid Peterson, Westinghouse Savannah River Company, P.O. Box 616, 773-A, Room B-132, Aiken, SC 29808
41. S. F. Piccolo, Westinghouse Savannah River Company, P.O. Box 616, 704-3N, Room S152, Aiken, SC 29808
42. Michael Poirier, Westinghouse Savannah River Company, P.O. Box 616, 679-T, Room 2A6, Aiken, SC 29808
43. J. M. Reynolds II, U.S. Department of Energy, Savannah River Operations Office, P.O. Box A, Building 704-196N, Room S441, Aiken, SC 29802
44. Jim Rindfleisch, Idaho National Engineering and Environmental Laboratory, Building 637, MS-5218, Idaho Falls, ID 83415-5218
45. K. J. Rueter, Westinghouse Savannah River Company, P.O. Box 616, 706-S, Room 103, Aiken, SC 29808
46. W. W. Schulz, 12704 Sandia Ridge Place NE, Albuquerque, NM 87111
47. Patricia C. Suggs, U.S. Department of Energy, Savannah River Operations Office, P.O. Box A, Building 704-196N, Room S431, Aiken, SC 29802
48. J. L. Swanson, 1318 Cottonwood, Richland, WA 99352
49. W. L. Tamosaitis, Westinghouse Savannah River Company, P.O. Box 616, 773-A, Room A-231, Aiken, SC 29808
50. Larry Tavlarides, Syracus University, Dept. of Chemical Engineering & Materials Science, 334 Hinds Hall, Syracuse, NY 13244-1190
51. T. A. Todd, Idaho National Engineering and Environmental Laboratory, Building 637, MS-5218, Idaho Falls, ID 83415-5218
52. George Vandegrift, Argonne National Laboratory, Building 205, 9700 South Cass Avenue, Argonne, IL 60439
53. Darrel D. Walker, Westinghouse Savannah River Company, P.O. Box 616, 773-A, Room B-124, Aiken, SC 29808
54. Dennis W. Wester, Pacific Northwest National Laboratory, P.O. Box 999, MS: P7-25, 902 Battelle Boulevard., Richland, WA 99352
55 J. H. Westsik, Pacific Northwest National Laboratory, P.O. Box 999, MS:K9-91, Richland, WA 99352
56 W. R. Wilmarth, Westinghouse Savannah River Company, P.O. Box 616, 773-42A, Room 153, Aiken, SC 29808
57 P. E. Woodall, U.S. Department of Energy, Idaho Operations Office, 750 DOE Place (MS 1145), Idaho Falls, ID 83402
58–64. Tanks Focus Area Technical Team, c/o B. J. Williams, Pacific Northwest National Laboratory, P.O. Box 999, MSIN K9-69, Richland, WA 99352
65. Tanks Focus Area Field Lead, c/o T. P. Pietrok, U.S. Department of Energy, Richland Operations Office, P.O. Box 550, MS: K8-50, Richland, WA 99352